



Universiteit  
Leiden  
The Netherlands

## Synthetic model microswimmers near walls

Ketzetzi, S.

### Citation

Ketzetzi, S. (2021, June 29). *Synthetic model microswimmers near walls*. *Casimir PhD Series*. Retrieved from <https://hdl.handle.net/1887/3185906>

Version: Publisher's Version

License: [Licence agreement concerning inclusion of doctoral thesis in the Institutional Repository of the University of Leiden](#)

Downloaded from: <https://hdl.handle.net/1887/3185906>

**Note:** To cite this publication please use the final published version (if applicable).

Cover Page



Universiteit Leiden



The handle <http://hdl.handle.net/1887/3185906> holds various files of this Leiden University dissertation.

**Author:** Ketzetzi, S.

**Title:** Synthetic model microswimmers near walls

**Issue date:** 2021-06-29

# 1

## Introduction

## Preface and Abstract

Initially aimed at mimicking and understanding biological swimmer behaviors, *synthetic microswimmers* have flourished on their own right, holding these days an important place within the newly found interdisciplinary field of *active soft matter*. A widely employed model system which at the same time has great potential for applications is that of *catalytically self-propelled* microswimmers. In this thesis, we examine the near-wall behavior of these model swimmers, which surprisingly remained to date largely unexplored, despite its high significance from both fundamental studies as well as applications perspectives.

In this chapter, we aim at providing a general introduction on microswimmers by presenting basic concepts as well as references for the interested reader. However, by no means do we mean to deliver an all-inclusive overview on microswimmers; considering the evergrowing literature, this task soon proved to be quite daunting. We focus for the most part on Pt-coated swimmers that catalytically propel themselves in hydrogen peroxide solutions, with emphasis on the seminal works that have led to their current understanding. We subsequently discuss open questions about this system and, in turn, conclude with the scope of this work.

From the moment we first open our eyes, the objects that capture our interest are the ones that move. The concept of motion for all its simplicity, and at the same time complexity, fascinates scientists and philosophers since the time of Aristotle. Motion constantly takes place all around us [1]: from animals and plants at the macroscale to bacteria and cells at the microscopic scale, all living organisms display numerous complex functions that are somehow intertwined with their motions, possibly leading to intricate patterns. We have all observed majestic patterns being formed when, e.g., looking at flocks of birds in the sky or schools of fish in the water. Intriguingly, these intricate patterns and complex behaviors that we may have seen in such systems at the group level, in actuality take place without a leader to organize them. Instead, these motions happen collectively [6].

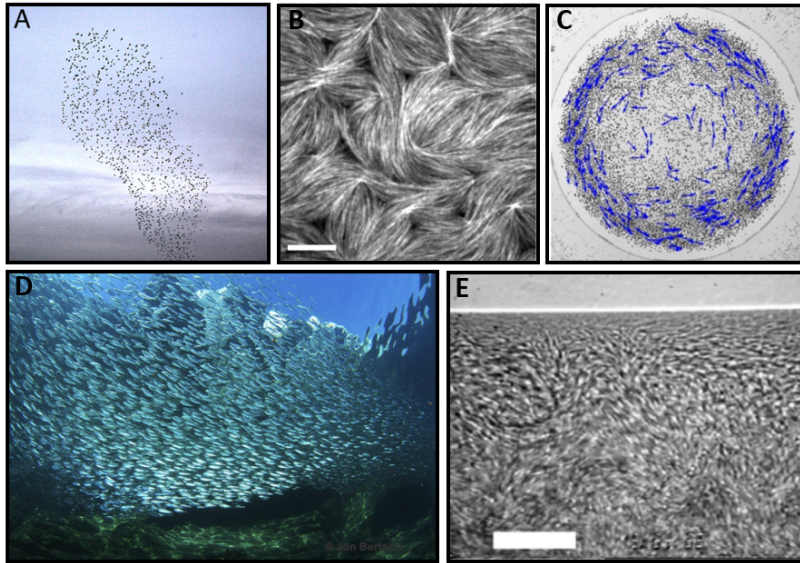


**Figure 1.1: Examples of active matter systems at the macroscopic (A, D) and microscopic (B, C, E) scale.** A) Flock of starlings *Sturnus vulgaris*; from Ref. [2]. B) Two-dimensional actomyosin network with nematic ordering, scale bar is 10  $\mu\text{m}$ ; from Ref. [3]. C) Colloidal rollers self-organized in a rotating vortex; from Ref. [4]. D) School of fish showing polar ordering. E) Bacterial turbulence in a sessile drop of *Bacillus subtilis*; scale bar is 35  $\mu\text{m}$ . D, E) Reprinted from Ref. [5] with permission from the American Physical Society.

Collective motion is the main focus of the highly interdisciplinary field of *active soft matter*, which investigates out-of-equilibrium behavior and processes that include, among others, motility-induced phase separation, flocking, and collective migrations [7]. Studies are performed on the macro- and microscopic scales both on biological, *e.g.* birds, bacteria, cells and cytoskeleton components such as actin networks, as well as synthetic systems, *e.g.* self-propelled colloidal particles, droplets, and swarming robots [8]. Figure 1.1 shows prominent examples of such systems. Irrespective of their size, these systems share the feature that their constituents, commonly referred to as particles, continuously dissipate energy from their environment into directed motion, or to exert mechanical forces, at their individual level [9]. In what follows, we restrict our focus to synthetic active matter in the microscale. For an overview of active matter systems at various length scales, we point the interested reader to the 2019 “Active Matter” Collections from *Nature* [10] and *Soft Matter* [11] and “The 2020 Motile Active Matter Roadmap” [12].

## Motion at the microscale

Motion of microorganisms in fluid environments is an absolutely crucial element of life. Through evolution, microorganisms have achieved robust and adaptive propulsion strategies that enable them to navigate efficiently in spatially or even time-varying environments, typically *via* different forms of taxis, *i.e.* motion in response to external stimuli [13]. For example, bacteria exhibit chemotaxis [14]: They move in response to chemical gradients which they utilize to find food or to avoid toxic substances. Sperm employ chemotaxis as well [15] in order to move towards the egg. But how do they propel themselves?

Due to their size,  $L$ , microorganisms in Newtonian fluids such as water, are subjected to low Reynolds ( $Re$ ) number hydrodynamics, with  $Re$  being defined as:

$$Re = \frac{\rho UL}{\eta} = \frac{UL}{\nu} \quad (1.1)$$

where  $\rho$  is the fluid density,  $U$  the flow speed,  $\eta$  and  $\nu$  the dynamic and kinematic viscosity respectively ( $\nu = 10^{-2} \text{ cm}^2/\text{s}$  for water). Thus,  $Re$

---

describes the relative importance of inertial and viscous forces [16]. Using reasonable dimensions for microswimmers like bacteria, i.e.  $L \approx 10 \mu m$  and  $U \approx 30 \mu m/s$ , we find  $Re \approx 10^{-4}$ . That is, motion is dominated by viscous forces. The dynamics of the (incompressible) fluid around the microswimmer is described by the Navier-Stokes equations:

$$\nabla \cdot \mathbf{u} = 0 \quad (1.2)$$

$$\rho \left( \frac{\partial \mathbf{u}}{\partial t} + (\mathbf{u} \cdot \nabla) \mathbf{u} \right) = \eta \nabla^2 \mathbf{u} - \nabla p + \mathbf{f} \quad (1.3)$$

where  $\mathbf{u}$  is the flow velocity,  $p$  the pressure and  $\mathbf{f}$  an external body force field. Following Refs. [17, 18], the non-linear contributions and inertial terms in Eq. 1.3 can be neglected when  $Re \ll 1$ , leading to the Stokes flow equation:

$$\nabla p - \eta \nabla^2 \mathbf{u} = \mathbf{f} \quad (1.4)$$

Equation 1.4, referred to as creeping flow, is linear and time-independent, i.e. it is symmetric under time transformations, which has severe implications for microscale motion in accordance with Purcell's "Scallop theorem": in a Newtonian fluid, any microswimmer that would change its body into a certain shape and, subsequently, change it back into its original shape through reversed steps like a scallop ("reciprocal motion"), would not be able to swim at the microscale [17].

Indeed, microorganisms such as bacteria and sperm swim by breaking time-reversal symmetry [19], or else by performing non-reciprocal motion, typically through the use of flexible, whip-resembling structures known as flagella (hairs) attached to their body. For example, *E. coli* swim in the direction of their long body axis by a "run and tumble" type of motion [18]. Briefly, when in the "run" phase, the flagella, rotating counterclockwise, form a bundle and the bacterium moves forward. In the "tumble" phase, however, some flagella rotate clockwise and leave the bundle, causing the bacterium to reorient. This type of motion aids them to find gradients in the fluid, e.g. in concentration of chemicals, to which they react accordingly by adjusting the duration of the "run" phases. Another strategy followed by cells such as sperm with one flagellum, involves beating the flagellum in a snake-like motion. These are but a few examples of propulsion strategies allowing biological swimmers to successfully overcome the dominant viscous drag [20];

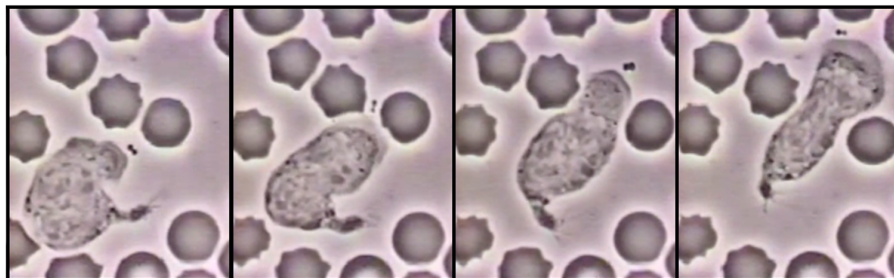


**Figure 1.2: Complex motion inside a complex environment.** These images are a set of snapshots adapted from a video taken by the late David Rogers at Vanderbilt University in the 1950's. The video, for which a blood film was adhered on a glass surface, shows a neutrophil (white blood cell) chasing a bacterium. The neutrophil constantly adjusts its shape to navigate its environment.

additional details on propulsion strategies adopted by diverse biological swimmers can be found in Ref. [18].

Biological swimmers are thus highly adaptable, resilient materials [21]: they assemble, regulate, and adjust themselves and their motility according to their environment. By further adapting to environmental conditions such as fluid flows, gravity and light, biological swimmers effectively navigate as well as perform complex tasks inside their fluid environments [13]. A great example is the neutrophil which adapts to its environment to catch the bacterium it senses in Figure 1.2. Overall, such intricate behaviors have inspired researchers to develop synthetic microswimmers, offering new opportunities for motion control at the microscale.

## Synthetic active matter

In recent years, self-regulation and propulsion, omnipresent in living materials [22, 23], have inspired the development of synthetic active materials [24]. The motivation for their development is twofold. On the one hand, synthetic microswimmers may serve as *model systems* for understanding out-of-equilibrium behaviors, in turn providing insights into biological microswimmers. Figure 1.3 shows that synthetic swimmers exhibit behaviors typically found in biological systems, as is for instance the formation of “living” crystals, seen for both colloidal surfers in Figure 1.3A and bacteria in Figure 1.3B. The strong resemblance to their bi-



ological counterparts justifies why researchers employ synthetic systems to gain insights into processes such as dynamic self-assembly, dynamic clustering and phase separation, as shown in Figures 1.4A and B.

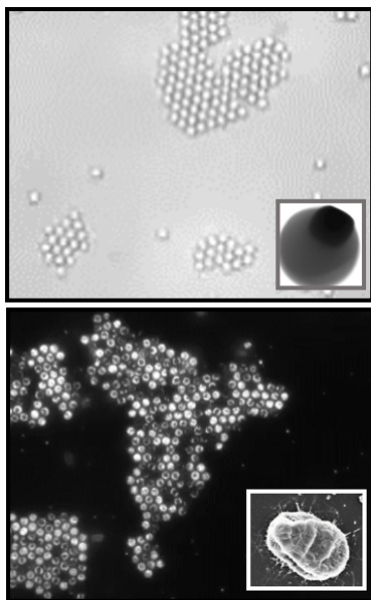


**Figure 1.3: Synthetic swimmers resembling biological microswimmer behaviors.** A) TPM-hematite colloidal surfers assemble into rotating crystals under blue light illumination. Adapted from Ref. [25] with permission from AAAS. B) *Thiovulum majus* bacteria self-organize into rotating crystals. Adapted from Ref. [26] (main panel) with permission of the American Physical Society and from Ref. [27] (inset).

On the other hand, model microswimmers are exceptional candidates for *applications* at the microscale, for example in biomedicine and microsurgery [28], where they could transport and deliver drugs at specific locations, or in environmental remediation [29], where they could locate and decompose pollution sources inside aquatic environments. Recent works in that direction are depicted in Figures 1.4C and 1.4D, showing that synthetic swimmers can indeed capture, transport, and release microcargo at different locations.

Thus, due to the far-reaching possibilities that they offer, intensive research has been dedicated to developing synthetic microswimmers which, in turn, has led to a variety of synthetic microswimmer systems becoming readily available within the past two decades. Notable synthetic systems nowadays include — but are not limited to — Pt half-coated catalytic swimmers [30] and bimetallic electrophoretic microrods [31] powered by chemical self-propulsion, Au half-coated thermophoretic swimmers powered by temperature gradients under laser ir-

radiation [32], Au-coated swimmers in water-lutidine mixtures powered by hydrophobic-hydrophilic interactions at the swimmer surface upon critical demixing of the solvent due to light irradiation [33], mag-

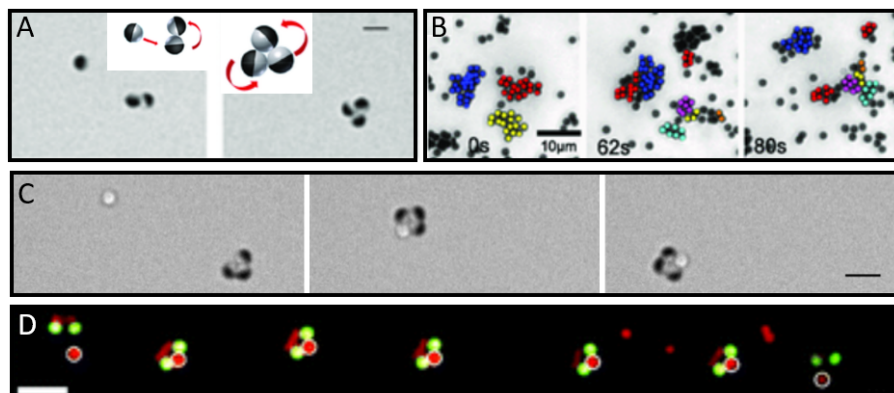


Figure 1.4: Synthetic microswimmers provide understanding of processes such as A) dynamic self-assembly and B) dynamic clustering and phase separation; scale bars are 2  $\mu\text{m}$  and 10  $\mu\text{m}$ , respectively. C) Transport of microscopic cargo by synthetic microswimmers; scale bar is 3  $\mu\text{m}$ . D) Capture, transport, and release of cargo; scale bar is 5  $\mu\text{m}$ . A, C) Adapted with permission from Ref. [43]. Copyright 2013 American Chemical Society. B) Reprinted from Ref. [44] with permission from the American Physical Society. D) Adapted from Ref. [45] with permission from the Royal Society of Chemistry.

netically [34] and acousto-magnetically [35] driven swimmers, swimmers powered by ultrasound [36], dielectric-Au swimmers driven by self-sustained electric fields using defocused laser beams referred to as opto-thermoelectric swimmers [37], light-activated surfers [25], colloidal rollers powered by Quincke electro-rotation [38], microscale Marangoni surfers at water-oil interfaces powered by asymmetric heating upon laser illumination [39], anisotropic Pt-coated swimmers with rough surfaces powered by periodic growth and bubble collapse [40], and swimming surfactant-stabilized liquid droplets powered by Marangoni stresses [41]. Note that propulsion in most of these systems relies at least in part on breaking the surface symmetry on the level of the swimmer, a swimming strategy first proposed by Ref. [42]. For the rest of the chapter, we restrict our discussion to catalytically self-propelled, and particularly to Pt half-coated swimmers, the model system studied in this thesis. For in-depth discussions on propulsion schemes, strengths, and weaknesses, of various synthetic systems we point the interested reader to some recent reviews on synthetic microswimmers [36, 46–51].

## Catalytic particles as model microswimmers

First coming into existence in the form of bimetallic microrods in hydrogen peroxide ( $\text{H}_2\text{O}_2$ ) solutions [31], catalytic microswimmers — or chemical swimmers as they are otherwise known — have nowadays become well-established model systems within the field of active matter. Two popular examples of catalytic swimmers, i.e. bimetallic microrods and dielectric-Pt Janus microspheres, are shown in Figure 1.5.

Unlike most systems mentioned in the previous section which are driven out-of-equilibrium with external light sources and fields, such particles are capable of truly autonomous motion, when suspended inside liquid environments often containing  $\text{H}_2\text{O}_2$  [54]. The reason why this ability is highly desirable over external actuation goes back to the applications microswimmers are intended for. As discussed in Ref. [13], adjusting swimmer dynamics externally could potentially become ineffective and/or impractical. That is, synthetic swimmers should ultimately propel within environments that may be temporally and/or spatially inhomogeneous, or even varying in completely unpredictable manners. Hence, external actuations would have to be continuously as well as thoroughly adjusted to match the time and length scales at hand [13].

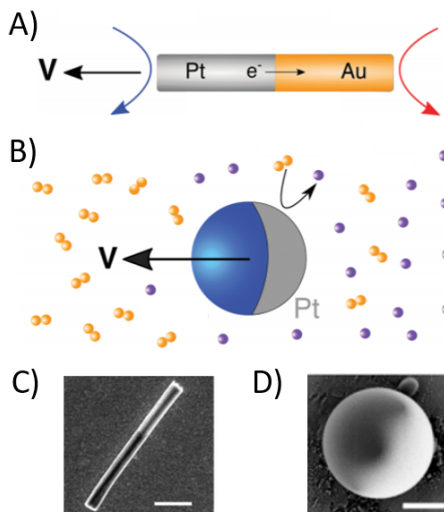


Figure 1.5: Examples of catalytic swimmers. **A)** Schematic representation of a bimetallic Pt-Au microrod. **B)** Schematic representation of a dielectric-Pt Janus sphere. **C)** Scanning electron microscopy (SEM) image of a Pt-Au rod. **D)** SEM image of a Pt-coated Janus sphere from our lab; the image is courtesy of Rachel Doherty. Scale bars are 1  $\mu\text{m}$ . A, B) Adapted from Ref. [52] with permission from The Royal Society of Chemistry. C) Adapted with permission from Ref. [53]. Copyright 2006 American Chemical Society.

Catalytic swimmers furthermore show relatively high propulsion speeds and can thereby be more efficient in their self-propulsion in comparison to other systems, see Ref. [46] for a comparison on the propulsion efficiency of various synthetic swimmers. In addition, catalytic swimmers exhibit tunability in their properties. For example, their speeds can be tuned upon changing system parameters [30, 55–58], as we will see in detail in the following section, while their motion can also be steered inside realistic environments comprising boundaries [59–61]. Lastly, they have shown a plethora of tactic behaviors, namely chemotaxis, phototaxis, gravitaxis, and rheotaxis, in response to stimuli in their environment, see Ref. [13, 62]. Altogether, these abilities provide large versatility and prospects in regulating their trajectories and overall behavior. Therefore, these particles are expected to prove useful in applications that require “smart” swimmers [13], i.e. swimmers that move autonomously across, as well as adapt accordingly inside, different environments.

### Self-phoretic motion

Unlike biological microswimmers which often achieve motion through time-asymmetric mechanical swimming, see the previous section, catalytic swimmers make use of short-ranged interactions between their surfaces and local gradients, which cause them to move through an effect known as *phoresis*. Phoresis is defined as the migration of microparticles caused by a gradient in some quantity inside a fluid medium; as Anderson has shown [63], gradients in concentration of solute molecules, electric potential, or temperature, lead to colloidal particle motion.

The motion of catalytic microswimmers uses the same principles, only in their case, it takes place due to *self-phoretic* effects instead. That is, the particles themselves generate gradients along their surfaces, and thereby instigate as well as maintain their own propulsion. In this section, following Ref. [64], we discuss general ideas behind the types of self-phoresis that are most commonly relevant for catalytic swimmers, namely, self-diffusiophoresis and self-electrophoresis [31].

To describe self-propulsion, models typically consider a particle inside a solvent that contains a dissolved solute phase [64]. The following set of equations is then used to describe the motion of the solute species  $i$ :

---


$$\frac{\partial c_i}{\partial t} + \nabla \cdot \mathbf{j}_i = 0 \quad (1.5)$$

$$\mathbf{j}_i = c_i \mathbf{u} - D_i (\nabla c_i + \frac{c_i}{k_B T} \nabla \psi_i) \quad (1.6)$$

with  $c$  the concentration,  $\mathbf{j}$  the flux in the dilute limit,  $D$  the diffusion coefficient,  $k_B$  the Boltzmann constant,  $T$  the absolute temperature, and  $\psi$  a generalized potential that describes the interaction of the solute with the environment. The respective terms in the right-hand side of Eq. 1.6 therefore describe — from left to right — the flux of the solute because of advection i.e. transport caused by the motion of the fluid, diffusion, and migration caused by the interaction potential [64]. As discussed in section 1, fluid flow in the low- $Re$  number regime is described by Eq. 1.2 and 1.4; here, the body force in Eq. 1.4 will depend on the interaction between the solute and the particle surface [64]. Equations 1.2 and 1.4-1.6 are generally employed to describe the motion of self-phoretic particles.

For simplification, theoretical studies often presume that phoretic effects are only manifested within an interfacial layer with thickness  $\lambda$  around the particle ( $\lambda/\alpha \ll 1$ , with  $\alpha$  the particle radius in Figure 1.6A) [65], typically referred to as the thin-layer approximation [66]. Moreover, they consider advection to be negligible compared to diffusion, i.e. the solute simply diffuses in the interfacial layer [67]. As discussed in Ref. [64], these assumptions eliminate the effect of the fluid flow on solute transport, while the solute concentration field still drives fluid motion through the body force. Finally, within the thin-layer approximation, the phoretic effects are represented by a slip velocity — proportional to the local gradient of  $\psi$  [68] — at the particle surface; the net velocity of the particle is then equal in magnitude and opposite in direction to the surface area average of the slip velocity [68, 69].

**Self-diffusiophoresis.** This type of propulsion has been suggested as relevant for the motility of actin and cells [70, 71] as well as for synthetic systems, see the following section. It is generated when a particle creates a concentration gradient of a solute and in turn moves in response to the forces created by the gradient. In the simplest case of neutral solute self-diffusiophoresis, the propulsion stems from a gradient of electrically-neutral solutes interacting with the particle, see Figure 1.6A

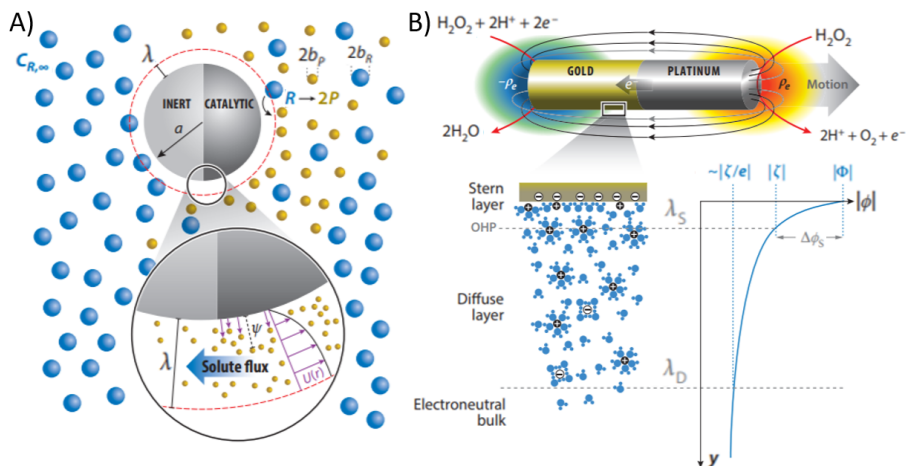


**Figure 1.6: Schematic illustrations of common self-phoretic propulsion types.** **A)** Neutral self-diffusiophoresis. The particle is a Janus colloid with two distinct hemispheres: the lighter hemisphere is the inert side, while the darker hemisphere is the catalytic side that drives the reaction. The catalytic side converts one reactant molecule (R, in blue) into two product molecules (P, in yellow). When the interaction between particle and molecules is repulsive, a phoretic flow occurs towards the catalyst, which causes the swimmer to move in the opposite direction, i.e. away from the catalyst. **B)** Self-electrophoresis. In Pt-Au microrods in  $H_2O_2$ , the Pt side oxidizes the  $H_2O_2$ , releasing electrons within the rod. These conduct to the Au side where they are consumed, creating water and protons into the fluid. The reactions generate as well as sustain an asymmetric charge distribution and, in turn, an electric field, causing a fluid flow around the particle that ultimately moves the particle towards the Pt side. A, B) Reprinted from Ref. [64] with permission from the Annual Reviews, Inc.

for a schematic. To model the reactions creating the gradient, models usually view the system from a macroscopic, i.e. continuum, perspective, and assume that the solutes are much smaller than the particle as well as omit the interactions between the solutes themselves (dilute limit). Solute transport is described by Eq. 1.5 and 1.6, with the interaction potential  $\psi$  within distance  $\lambda$  from the particle surface defined as  $\nabla\psi \equiv -\mathbf{f}_s$ , with  $\mathbf{f}_s$  the net force on a solute molecule [65]. Due to Eq. 1.4, the force on the solute transfers to the fluid, causing  $\mathbf{f} = -c\nabla\psi$  on the fluid. According to Anderson [63], the neutral self-diffusiophoretic particle velocity,  $U_d \propto \nabla c$ .

---

The most commonly used potential in neutral-diffusiophoresis [72] is the excluded volume — or else hard-sphere — potential, i.e. strong repulsion at contact, while others, such as the exponential or van der Waals potentials have also been used in self-diffusiophoresis [73]. See Ref. [64] for discussions on interaction potentials as well as a review on constant flux versus reaction kinetic models in theoretical diffusiophoretic studies.

**Ionic self-diffusiophoresis.** This propulsion type is relevant for swimmers whose surface reactions produce both anions and cations [74]. It has been recently discussed in view of synthetic swimmers in  $\text{H}_2\text{O}_2$  solutions, see Refs. [74–76] for in depth discussions. It is conceptually similar to neutral self-diffusiophoresis, however the fluid flow that propels the particles is in this case a result of free ionic species interacting with their surface [75]. Although ions are not present in  $\text{H}_2\text{O}_2$  decomposition ( $2\text{H}_2\text{O}_2 \rightarrow 2\text{H}_2\text{O} + \text{O}_2$ ),  $\text{H}_2\text{O}_2$  may undergo ionic disassociation ( $\text{H}_2\text{O}_2 \rightleftharpoons \text{HO}_2^- + \text{H}^+$  [75]) which could result in an ionic gradient that ultimately produces tangential fluid flow along the particle surface. In ionic self-diffusiophoresis, ions interact with a charged particle surface through Coulomb interaction. Although the fluxes of positive and negative ions (here,  $\text{H}^+$  and  $\text{HO}_2^-$ , respectively) are equal, i.e. there is no electrical current, the two ions may diffuse at different rates [74]. For unequal ion diffusion rates, and to maintain bulk charge neutrality [75], a (diffusion) potential is created to prevent net charge separation.

**Self-electrophoresis.** This type of propulsion occurs for a variety of synthetic particles whose surface consists of two metals. As mentioned earlier, the first example is that of Pt-Au rods [31] but it is also applicable to various bimetallic particles, see Ref. [53] for more examples, as well as spheres [77]. A requirement for this propulsion type is that the surface of the particle is charged. In electrolyte solutions, the charged surface attracts ions carrying opposite surface charge — named counterions — which causes a layer of immobile counterions around the particle to form, called the Stern layer (Figure 1.6B). Outside this layer, there exists a second layer, the diffuse screening layer, of both negatively and positively charged ions, depending on the position within the layer; at the end of the diffuse screening layer, negatively and positively charged ions are equally distributed, see also Figure 1.6B. Together, these two layers constitute the electric double layer (EDL) whose thickness is known as the Debye length,  $\lambda_D$ . When, e.g., Au-Pt particles are suspended in a  $\text{H}_2\text{O}_2$

solution, electrochemical reactions cause ion exchange between their surface and the solution, see Figure 1.6B. In that system,  $\text{H}_2\text{O}_2$  is oxidized at the Pt end producing protons and electrons, and, *vice versa*, reduced at the Au end [53], establishing a gradient in the concentration of charges. This asymmetry in the charge distribution results in an electric dipole around the particle which, in turn, creates an electric field that couples to the ions in the EDL [64], causing a body force in the fluid and thereby the fluid to move with respect to the particle. Hence, the particle moves in the direction of the Pt end. This process is equivalent to electrophoresis, although similar to our previous discussion on self-diffusiophoresis, the flux of charges and resulting electric field is again created by the particle itself. Specifically, ion transport is here also described by Eq. 1.5, while the flux  $\mathbf{j}$  in Eq. 1.6 additionally depends on electromigration with the interaction potential given by  $\psi_i = z_i e \phi$ , with  $z_i$  the species and  $e$  the elementary charge. The particle-generated electric field  $E = -\nabla \phi$  exerts on the fluid the body force  $\mathbf{f} = \rho_e \nabla \phi$ , with  $\rho_e$  the volumetric charge density, causing the fluid and, in turn, the particle to move with the self-electrophoretic speed  $U_e \propto \zeta E$  where  $\zeta$  is the particle zeta potential relating to its charge [78]. For details on flux-based as well as reaction-kinetic models in theoretical self-electrophoretic studies see Ref. [64].

## Pt-coated Janus swimmers

We now turn to Pt-coated Janus microparticles, the focus of this thesis. Pt-coated particles a few micrometers in diameter constitute a prominent microswimmer system that has received a lot of attention since its establishment by Ref. [30] in 2007. The reason why such particles are highly interesting is that they exhibit truly autonomous motion inside  $\text{H}_2\text{O}_2$  as well as they have great potential for adaptability. Hence, these properties make them important candidates for applications in the microscale. We point the interested reader to Ref. [54] for a discussion on the technological relevance and advantages of Pt-coated microswimmers from the perspective of applications. We note however that a challenging aspect which still remains to be tackled is their biocompatibility relating to their solvent toxicity, although there are some promising studies on bimetallic nanojets with epithelial cells [48, 79] and more recently on pH-responsive catalytic motors in varying lactic acid conditions [80].



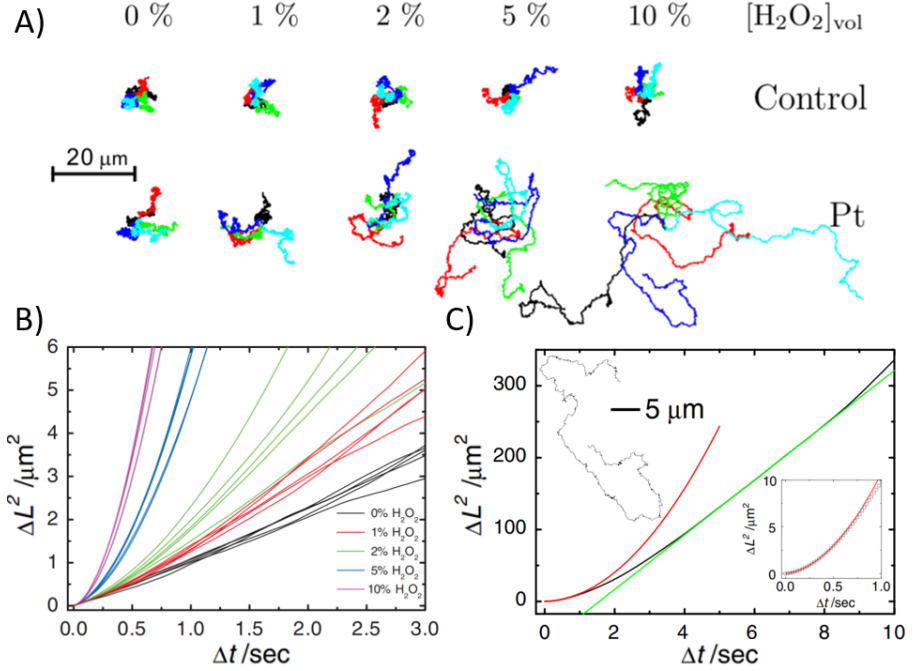


**Figure 1.7: Self-propulsion of Pt-coated swimmers in  $\text{H}_2\text{O}_2$  solutions.** A) Unlike the uncoated (control) particle which exhibits Brownian motion for the same  $\text{H}_2\text{O}_2$  conditions (top), Pt-coated particles perform directed motion with increasing  $\text{H}_2\text{O}_2$  concentration (bottom). B) The particle mean square displacement (MSD) as a function of time changes from linear at 0%  $\text{H}_2\text{O}_2$  (in black) to parabolic with  $\text{H}_2\text{O}_2$  concentration. C) The MSD of a single particle resembles a parabola at short-time scales (in red), and a straight line (in green) at time scales much larger than the timescale for particle rotation. The inset shows a single particle trajectory (left) and the short-term MSD regime (right). All panels are reproduced from Ref. [30] with permission from the American Physical Society.

Figure 1.7 shows several key findings describing the self-propelled motion of Pt-coated particles in  $\text{H}_2\text{O}_2$  solutions. In their pioneering experiments, Howse *et al.* verified the predictions of Ref. [42], which proposed that propulsion can be achieved by asymmetric distribution of reaction products, by demonstrating that Pt-coated particles exhibit directed motion in  $\text{H}_2\text{O}_2$  solutions (Figure 1.7A). They found that particles cover larger distances over the same time with increasing  $\text{H}_2\text{O}_2$  concentration,

as also reflected in the mean square particle displacements (MSDs) of Figure 1.7B. Moreover, they showed that the particle MSD can be decomposed into a short-term ballistic part and a long-term diffusive part, either of which can be fitted with appropriate expressions to provide the particle velocity. We return to the short-term behavior and corresponding MSD expression in chapter 2, where we provide an in-depth discussion on its nature and applicability. Lastly, in line with Figure 1.7B, Howse *et al.* were the first to report that particle velocity initially increases and thereafter plateaus with  $\text{H}_2\text{O}_2$  concentration, see Figure 1.8A.

Since then, research has shown that the velocity of Pt-coated swimmers depends on several parameters, in addition to the  $\text{H}_2\text{O}_2$  concentration, as shown in Figure 1.8. Ref [55] showed that particle velocity increases almost linearly with the thickness of the catalytic Pt layer, see red curve in Figure 1.8B named PVD after the term “physical vapor deposition” which is the standard way of coating the particles with Pt. The same work proposed an alternative way of preparing Pt-coated Janus particles in which the Pt is grown on the particle in solution. Particles prepared following their method also show Pt-thickness-dependent velocities, see the blue curve in Figure 1.8B. Moreover, swimming velocities depend upon the particle surface slip, as demonstrated by the experiments of Ref. [56], which employed otherwise similar particles with varying surface hydrophobicity, see also Figure 1.8C. This figure shows that velocity increases with  $\text{H}_2\text{O}_2$  concentration, similar to Ref. [30] — although velocities here plateaued at a lower  $\text{H}_2\text{O}_2$  concentration — while at the same time they reported an appreciable increase in the velocity for the hydrophobic (in black) in comparison to the hydrophilic (in red) particles. This effect was more pronounced for their larger particles of  $5.2\text{ }\mu\text{m}$ , while noting that these particles always moved considerably slower than their  $2\text{ }\mu\text{m}$  particles. This result was in line with the particle velocity notably decreasing with size, as found in the experiments of Ref. [58] in Figure 1.8D, wherein it was first established that swimming velocity scales inversely with swimmer size. Ref. [58] attributed this decrease to the intrinsic features of the self-diffusiophoretic propulsion mechanism.

Apart from tunable velocities, another key feature of Pt-coated swimmers is their affinity for surfaces. Pt half-coated particles depending on their mass density tend to swim upwards and/or downwards until they reach the top and/or bottom of their container, and thereafter remain there, self-

propelling parallel to their container wall. Figure 1.9A shows a video microscopy measurement of a Pt-coated swimmer that has settled above the bottom wall (substrate), moving in two dimensions with its Pt side at the back at all times [81]. This work also showed for the first time that the velocity vector corotates with the orientation of the swimmer, i.e. that the orientation of the Pt and the direction of motion are correlated. Ref. [81] additionally discussed that the direction of motion eventually becomes randomized as Brownian diffusion acts as noise, in line with the short-term and long-term behavior of the MSD from Ref. [30]. Thus, the active motion enhances the diffusion rate of the particles, with the ex-

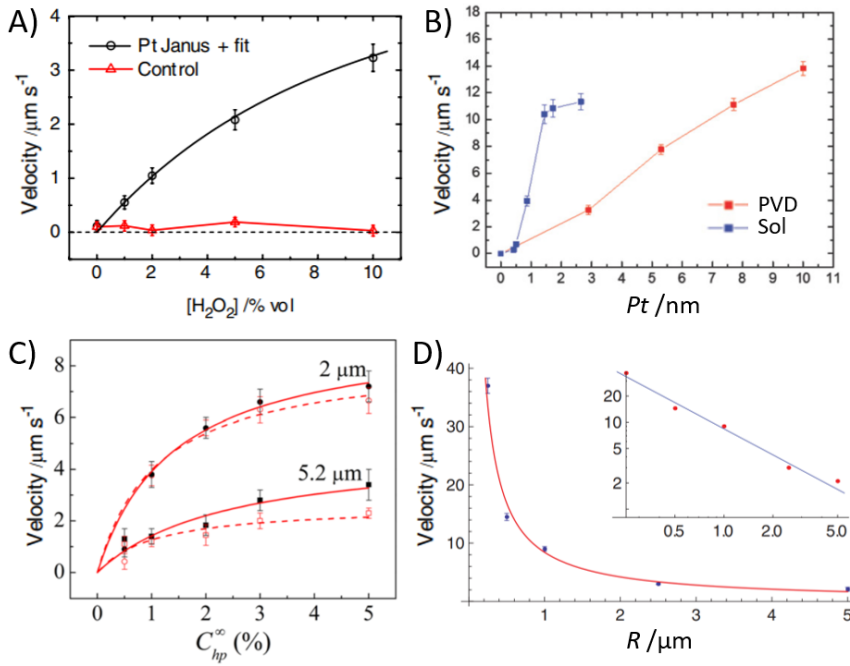


**Figure 1.8: Parameters affecting the swimming velocity of Pt-coated swimmers in  $\text{H}_2\text{O}_2$  solutions.** These findings are compatible with self-diffusiophoresis. **A)** Velocity increases with  $\text{H}_2\text{O}_2$  concentration [30]. **B)** Velocity increases with Pt-coating thickness; adapted from Ref. [55]. **C)** Velocity increases with the hydrophobicity of the swimmer surface, in addition to its increase with  $\text{H}_2\text{O}_2$  concentration [56]. **D)** Velocity scales inversely with swimmer size [58]. Adapted with permission of A, D) the American Physical Society and C) AIP Publishing.

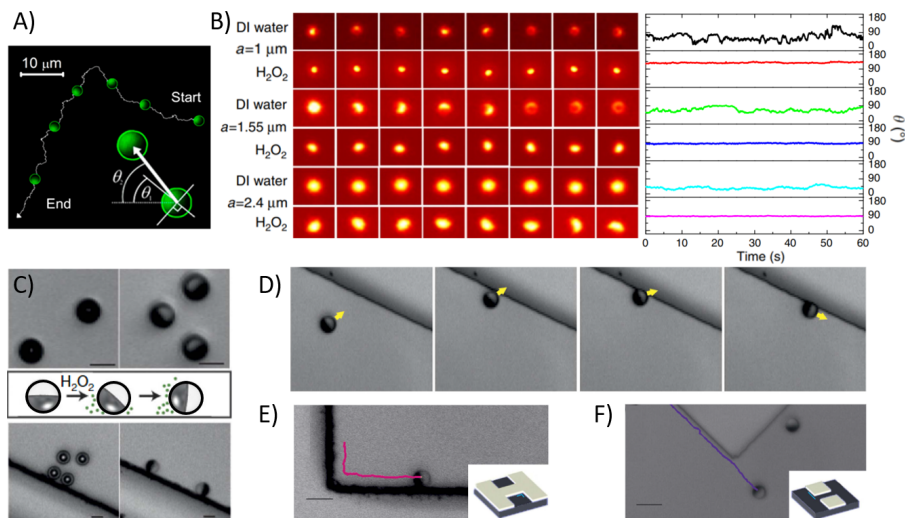


**Figure 1.9: Affinity of Pt-coated swimmers for surfaces: swimmer alignment and potential for guidance.** **A)** The swimmer moves away from its Pt side and over the same plane above the bottom wall of the container (substrate) [54, 81]. Reprinted with permission from Ref. [54]. Copyright 2018 American Chemical Society. **B)** The particles rotate freely in water, with rotation being slowed down with size, as shown in the fluorescent images of rows 1 (radius 1  $\mu\text{m}$ ), 3 (radius 1.55  $\mu\text{m}$ ), and 5 (radius 2.4  $\mu\text{m}$ ) (left), as well as in the corresponding fluctuating angles formed between the Pt-coating and substrate (right). In  $\text{H}_2\text{O}_2$ , the same particles show a steady orientation relative to the substrate, see the images in rows 2 (radius 1  $\mu\text{m}$ ), 4 (radius 1.55  $\mu\text{m}$ ), and 6 (radius 2.4  $\mu\text{m}$ ), and corresponding constancy in the angles (on the right), for all swimmer sizes; adapted from Ref. [59]. **C)** Bottom-heavy particles in water tend to orient themselves with the Pt cap facing down (top left), while they orient their caps vertically with respect to the wall upon addition of  $\text{H}_2\text{O}_2$  instead (top right). In water, the particles diffuse near a secondary wall that is placed vertical to the substrate (bottom left), while in  $\text{H}_2\text{O}_2$  they slide along the vertical wall (bottom right). **D)** In  $\text{H}_2\text{O}_2$ , when the swimmers approach a vertical wall, they reorient their axis and slide along the wall, with their cap oriented vertically to both the secondary wall and substrate. This surface affinity can be used to guide the motion of the swimmers. **E)** A swimmer can follow a 90 deg corner, while in **F)** it cannot do the same for a reflex angle of 270 deg, with the corresponding insets showing the schematics of the structures used in the experiments. C-F) Reprinted from Ref. [60].

---

pectation being that smaller swimmers will become diffusive faster while larger swimmers will have persistent directionalities [81].

Regarding swimmer orientation with size, Ref. [59] showed that swimmers irrespective of size have a preferred orientation with the substrate, with larger particles having a steady state orientation of 90 deg in agreement with Ref. [81], as shown in Figure 1.9B. In comparison, in the same figure, the same particles show large fluctuations in orientation above the substrate when suspended in pure water. Thus, orientational locking happens only in the active state of the particles in  $\text{H}_2\text{O}_2$  [59]. The same behavior was at the same time also observed in the experiments of Ref. [60], see also Figure 1.9C where the particles change their orientation upon addition of  $\text{H}_2\text{O}_2$ . Their activity also keeps the particles in motion relative to secondary vertical walls, see bottom of Figure 1.9C and Figure 1.9D, where the swimmer is clearly seen to adjust its orientation with respect to the wall. Sliding at a constant orientation is observed along vertical walls, a feature additionally explored in more complicated geometries for the prospect of guiding swimmers to additionally avoid the randomization of their motion due to Brownian noise. Ref. [60] showed that although swimmers can follow 90 deg corners, they cannot follow 270 deg corners, see Figures 1.9E and 1.9F, respectively, as well as that swimmers cannot go over steps depending on their heights, see Ref. [60]. That is, a step of height larger than a few hundred nanometers will stop a swimmer from going over it. Based on these observations, employing topographical features has been proposed as a useful strategy for directing motion and increasing motion persistence in the microscale.

Another strategy that leads to modifications in their trajectories is changing the surface coverage by the catalyst. This can be achieved in a controlled way when the particles are deposited in a crystal lattice during Pt sputtering [54, 82], see also Figure 1.10A. Controlling the geometry and hence portion of the catalyst results in angular motion and/or spinning motion that may be useful for certain applications. Finally, during self-propulsion single spheres may self-assemble into dimers. Ref. [83] showed that different relative sphere orientations yield differences in the curvature of the trajectory of the assembled dimer. Although useful as a means to modify active trajectories, the configurations resulting from activity-induced self-assembly are random and thereby this process does not offer precise control. To date, employing nonspherical particles with

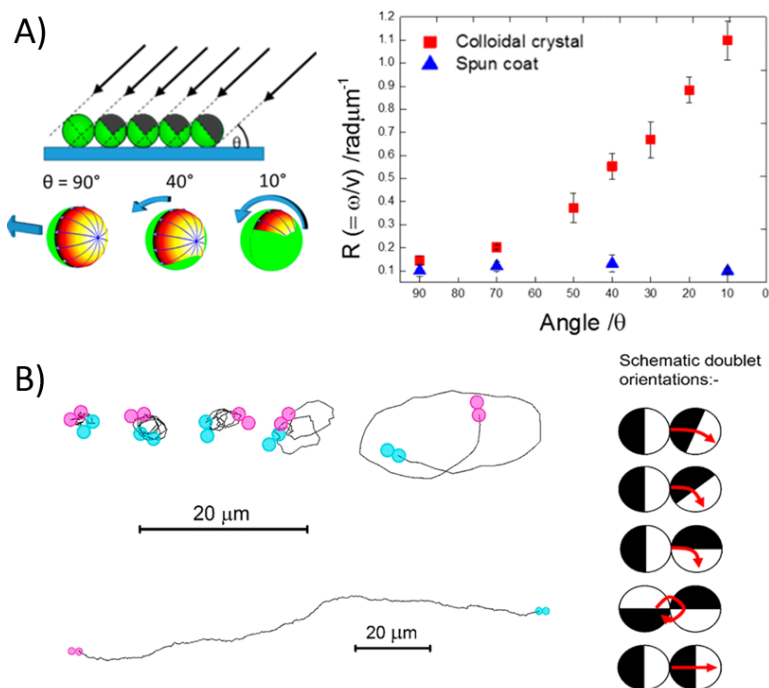


**Figure 1.10: Tuning Pt-coated swimmer trajectories.** A) Asymmetric coatings can be applied by varying the sputtering deposition angle when the particles are packed in 2-dimensional crystals [54, 82]. This simple technique can be used to tune the ratio between their translational and rotational velocity. B) The swimmer trajectory can be tuned from linear to highly curved by forming dimers through the active assembly of single swimmers [54, 83]. Different relative orientations of the swimmers result in trajectories with varying degrees of curvature, although precise control over the trajectory is not possible due to the random nature of the active self-assembly process. A, B) Reprinted with permission from Ref. [54]. Copyright 2018 American Chemical Society.

well-defined configurations is experimentally relatively unexplored. Although all existing experiments show that deviations from the spherical shape result in curved trajectories [84–88], controlled experiments that identify the effect of microswimmer shape are still desirable.

## Open questions

Despite Pt-coated particles in  $\text{H}_2\text{O}_2$  being a seemingly simple active system with great potential for adaptable autonomous motion, there are still several open questions and puzzling observations pertaining to it. Although the findings described earlier in this section are generally compatible with the self-diffusiophoretic mechanism originally proposed for this system [30], the behavior of these swimmers in the presence of salts and anionic surfactants is not commensurate with it. That is, the speed of Pt-coated swimmers considerably decreases upon addition of salt and certain surfactants in solution. This finding was first reported by Brown *et al.* [75] and Ebbens *et al.* [76], see also Figures 1.11A and B, respectively.

In their original experiments, Howse *et al.* proposed that Pt-coated particles propel themselves according to self-diffusiophoresis by creating gradients of molecular oxygen along their surfaces, which are the products of the  $\text{H}_2\text{O}_2$  decomposition on the Pt end [30]. However, a few years later in 2014, Brown and Poon [75] as well as Ebbens *et al.* [76] reported ionic effects on the motion of Pt-coated swimmers. In addition, Brown and Poon [75] discussed that direction reversals have also been observed

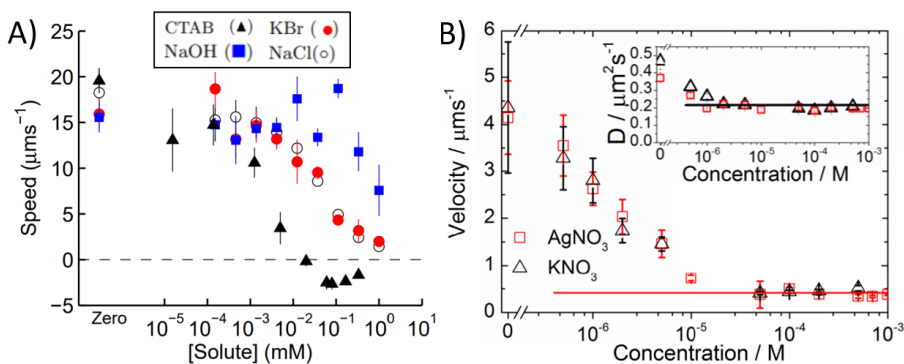


**Figure 1.11: Ionic effects on the speed of Pt-coated swimmers.** A) Swimming speed decreases when the concentration of ionic compounds such as NaOH, salts (NaCl and KBr) and surfactants (CTAB) increases from 0 and 1 mM. B) Similarly, swimming speed decreases when the concentration of salts ( $\text{KNO}_3$  and  $\text{AgNO}_3$ ) increases from 0 and 1 mM, while their diffusion coefficient remains constant between concentrations of 1  $\mu\text{M}$  and 1 mM. Image adapted from Ref. [76]. Adapted from A) Ref. [75] with permission from The Royal Society of Chemistry.

in catalytic systems. Both references concluded that self-diffusiophoresis cannot be the only mechanism at play. Brown *et al.* discarded the possibility that the swimmers move due to ionic self-diffusiophoresis on the basis that the observed particle velocities would require that the particles had unusually large surface zeta potentials. As a consequence, they suggested self-electrophoresis as the mechanism behind the observed behavior [75]. Although this mechanism requires two metallic ends such that there is a difference in their electron affinity, see discussion in the previous section, it was proposed that asymmetries in the Pt coating layer due to its preparation — the Pt at the pole can be thicker than the Pt at the equator of the particle surface — could cause differences in the reaction rates along the Pt end. That is, the asymmetry in the reaction rate suffices to generate a current along the particle. This was later investigated and deemed possible also from a theoretical perspective by Ibrahim *et al.* [89]. Note that all works discussed so far concerning propulsion mechanisms assume that swimming takes place in the bulk of the fluid.

Moreover, it is important to notice that discrepancies in swim speeds are often found in the literature for Pt-coated swimmers, even under similar conditions. For example, Ref. [30] measured that polystyrene particles of  $1.6\text{ }\mu\text{m}$  in diameter with a  $5.5\text{ nm}$  thick Pt layer self-propelled at  $\approx 3\text{ }\mu\text{m/s}$  in  $10\%$   $\text{H}_2\text{O}_2$ . On the other hand, polystyrene particles of  $2\text{ }\mu\text{m}$  in diameter with a  $5\text{ nm}$  thick Pt layer self-propelled on average at  $\approx 18\text{ }\mu\text{m/s}$  in  $10\%$   $\text{H}_2\text{O}_2$ . Taking into account what we have learned from Figure 1.8 on the parameters affecting swim speeds, this discrepancy is unexpected. That is, for the same  $\text{H}_2\text{O}_2$  concentration and particle material, i.e. particle slip, we expect similar velocities. Even more so, the combination of the smaller size as well as relatively thicker Pt layer in Ref. [30] should have resulted in larger speeds in comparison to Ref. [75], opposite of what was measured. In fact, taking a closer look at the  $0\text{ mM}$  data points of Figure 1.11A (data in the absence of salt), we notice that speed measurements by the same researchers on the exact same particles range from an average of  $15\text{ }\mu\text{m/s}$  to an average of  $20\text{ }\mu\text{m/s}$ . This already suggests that additional factors contribute to the experimentally measured swim speeds. Overall, the above demonstrate that the current picture of catalytic self-propulsion and speed-affecting parameters is not yet complete.



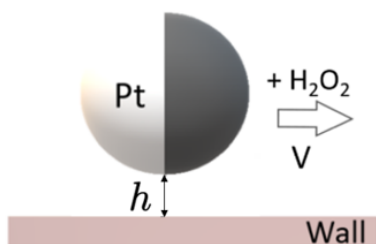
---

## Scope of this thesis

To date, confining surfaces are known to have striking effects on the motion of microorganisms [18]. For example, surfaces can significantly modify swimming trajectories of biological swimmers: bacteria having high surface affinity tend to accumulate on walls, where they often exhibit circular motion with direction controlled by the boundary condition [90–93], in stark contrast to their run-and-tumble motion in bulk.

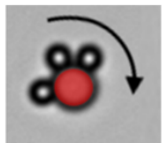
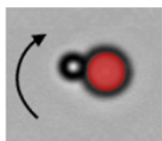
Seeing that Pt-coated swimmers likewise share the affinity for walls, and since their motion is typically measured near a wall, it is natural to question how, and to what extent, walls influence their motion. Surprisingly, when we were starting the work presented in this thesis, little to no research had focused at the time on the effects of the wall, in spite of walls already being considered as a means to guide active motion. That is, in interpreting as well as modeling catalytic microswimmer experiments, swimming was assumed to take place in bulk. However, understanding wall effects is important both for the use of Pt-coated swimmers as models systems as well as from the perspective of applications, since these swimmers are intended to perform tasks in complex environments where ultimately confining surfaces will be present. For the aforementioned reasons, this thesis focuses for the most part on exploring the effects that walls have on catalytic microswimmer motion.

In **chapter 2**, we consider the effect of a planar wall on the motion of Pt-coated swimmers. By performing experiments on the same particle batch above substrates made of various materials, we found that walls indeed have a strong effect on their swimming speeds. That is, walls other than glass which had typically been used in the experiments are capable of speeding up or slowing down particle motion. This effect can be attributed to an interplay between the hydrodynamic boundary



condition on the wall, set by its slip, and the out-of-equilibrium chemical species generated by the swimmer, through an osmotic coupling mechanism. These findings provide a path towards resolving conflicting experimental observations regarding disparate swimmer speeds.

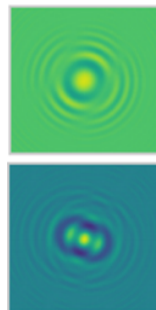
In **chapter 3**, motivated by our previous findings, we develop a method based on diffusion analysis to measure swimmer-wall separations. Using this method, we found that Pt-coated swimmers propel at  $\approx 300$  nm from the wall, in agreement with observations of them not being able to propel over steps of a few hundred nanometers and with the wall-dependent speed findings. Moreover, we found that swimmers assume fixed heights above the wall for a range of salt concentrations, swimmer surface charges, and swimmer sizes, which we call “ypsotaxis”. Finally, our experiments in the presence of salt provide novel insights on the debated propulsion mechanism: the speed decrease may stem from long-range  $\text{H}_2\text{O}_2$  gradients acting on the wall on the basis of an ionic diffusioosmosis mechanism along the wall, which creates a flow that counteracts swimmer motion. Nearby walls are thus dominant factors in controlling swim speeds and should be taken into account in future modeling.



In **chapter 4**, we furthermore restrict Pt-coated swimmers to move along closed 1-dimensional paths. While single swimmers move at stable speeds independent of path curvature, multiple swimmers along the same path move at higher speeds depending on the swimmer number. At the same time, the swimmers keep at preferred distances due to an effective activity-induced potential stemming from a competition between chemical and hydrodynamic coupling. Swimmers also actively assemble into trains as well as compact chains with highly dynamic behaviors

depending on path curvature. These findings open the door towards exploiting cooperation for applications inside complex environments.

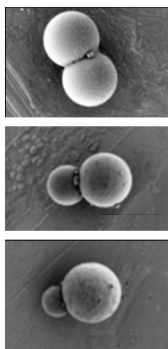
In **chapter 5**, we develop a method for measuring non-coated particle-wall distances based on holographic microscopy. First, we employ it on spheres to crosscheck our diffusion-based height analysis method of chapter 3. Second, we employ it to colloidal dumbbells of different sizes to measure their height-dependent orientation with the wall, and gain insights into the largely unexplored near-wall dynamics of nonspherical microparticles. We found that dumbbell orientation with respect to the wall changes with size. At specific heights both net forces and torques on the dumbbells are simultaneously below the



---

thermal force and energy, respectively, making the observed orientations possible. These results may prove useful for developing quantitative frameworks for arbitrarily shaped particle dynamics in confinement.

In **chapter 6**, motivated by the need for finely tuning catalytic swimmer trajectories for applications, as well as inspired by microorganisms whose shapes often enable them to navigate complex environments, we aimed at exploring the effect of swimmer shape on its self-propelled motion. To this end, we studied the motion of Pt-coated dumbbell-shaped swimmers



with varying degree of asymmetry near walls. We find that self-propelled dumbbells move parallel to the wall, with trajectories that depend upon their shape and coating: increasing particle asymmetry leads to pronounced circular motions. We compare the radius of particle trajectories from our measurements to existing theory on asymmetric self-propelled particles near a wall, and find good agreement, confirming that the radius of circular motion depends on particle shape and coating. Our findings may prove useful for increasing swimming directionality and, in turn, motion control in complex environments.

